INTERNATIONAL JOURNAL OF CLIMATOLOGY
Int. J. Climatol. (2015)
Published online in Wiley Online Library
(wileyonlinelibrary.com) DOI: 10.1002/joc.4244

RMetS
Royal Meteorological Society

The alleviating trend of drought in the Huang-Huai-Hai Plain of China based on the daily SPEI

Qianfeng Wang,[a,b] Peijun Shi,[a] Tianjie Lei,[a,b] Guangpo Geng,[a,b] Jinghui Liu,[a,b] Xinyu Mo,[a,b] Xiaohan Li,[a,b] Hongkui Zhou[a,b] and Jianjun Wu[a,b]*

[a] *Academy of Disaster Reduction and Emergency Management, Ministry of Civil Affairs and Ministry of Education, Beijing Normal University, China*

[b] *Center for Drought and Risk Research, Beijing Normal University, China*

ABSTRACT: Drought is a major natural hazard that can have devastating impacts on regional agriculture, water resources and the environment. To assess the variability and pattern of drought characteristics in the Huang-Huai-Hai (HHH) Plain, the daily Standardized Precipitation Evapotranspiration Index (SPEI) is developed based on daily meteorological data in this study. The daily SPEI data are used, including Annual Total Drought Severity (ATDS), Annual Total Drought Duration (ATDD) and Annual Drought Frequency (ADF), which were calculated from 1981 to 2010 at 28 meteorological stations. We used the indices (ATDS, ATDD and ADF), Hovmöller diagrams and the reliable no parameter statistical methods of the Mann–Kendall test to assess the variability and pattern of drought characteristics for the period from 1981 to 2010 in the HHH plain. The results suggested that severe drought occurred in the 1980s, the late 1990s and the early 2000s, severe drought events occurred in 1981, 1986, 1997 and 2002. Decreasing trends for both ATDS and ATDD were found, and the drought situation did not worsen under global warming during the past 30 years, and the drought situation is alleviating in the entire HHH plain. The northeast and southwest regions of the HHH plain have suffered from more severe drought, and the north region is prone to drought. The results of the study can provide a scientific understanding for the adoption of countermeasures of regional defence against drought and also may serve as a reference point for drought hazard vulnerability analysis.

KEY WORDS variability; pattern; drought; SPEI; Huang-Huai-Hai Plain

Received 1 October 2014; Revised 2 December 2014; Accepted 2 December 2014

1. Introduction

Drought is one of the costliest natural disasters (Wilhite, 2000; He *et al.*, 2011), and it is also the most complex and the least understood natural disaster that affects humans (Hagman *et al.*, 1984; Wilhite, 1996). The number of severe drought events and the drought duration are likely to increase (Blunden *et al.*, 2011; Li *et al.*, 2011). In particular, severe drought can have devastating effects (Shen *et al.*, 2007), such as exacerbated and intensified environment degradation and desertification, serious stoppage of river flow, loss of socio-economically significant crop yield, increased risk of forest fires, and increased competition for resources and social violence (Bruins and Berliner, 1998; Quiring and Papakryiakou, 2003; Pausas, 2004; MacDonald, 2007; Zhang *et al.*, 2014). In 1997, a drought resulted in 226 days of zero flow in the Yellow River from Henan to Shandong provinces (Liu and Zhang, 2002; Wang *et al.*, 2011); in 2002, 26 states in the United States were affected by severe and extreme drought, with total losses exceeded $2.7 billion (Wilhite *et al.*, 2007). Thus, the effects of drought have recently evoked interest beyond the scientific community (Leuzinger *et al.*, 2005).

The current common drought monitoring indices include the SPI (Standardized Precipitation Index), PDSI (Palmer Drought Severity Index), ISDI (Integrated Surface Drought Index), SPEI (Standardized Precipitation Evapotranspiration Index), TCI (Temperature Condition Index), VCI (Vegetation Condition Index) and the VHI (Vegetation Health Index) (Rhee *et al.*, 2010; Banimahd and Khalili, 2013; Wu *et al.*, 2013; Hu *et al.*, 2014); the SPEI (Vicente-Serrano *et al.*, 2010; Wang *et al.*, 2014); the SPI (McKee *et al.*, 1993) and the PDSI (Palmer, 1965) are the three most widely used drought indices. The results of using the SPI are comparable in space and time (Guttman, 1998; Hayes *et al.*, 1999), and their multi-scale characteristics can identify different types of droughts. However, the SPI only considers the precipitation factor, which does not reflect drought conditions caused by warming. The PDSI reflects the drought effects caused by warming (Dubrovsky *et al.*, 2009), and the trends in drought areas have been investigated based on the PDSI on a global scale (Sheffield *et al.*, 2012). Although the PDSI takes temperature factors into account, it lacks the multi-scale characteristics that are necessary for the evaluation of different types of drought. Taking the multi-scale convenience of the time and temperature effects for

* Correspondence to: J. Wu, Academy of Disaster Reduction and Emergency Management, Ministry of Civil Affairs and Ministry of Education, Beijing Normal University, Beijing, China. E-mail: jjwu@bnu.edu.cn.

drought assessment into account, the SPEI is very suitable for monitoring and researching drought characteristics under warming, and there have already been some studies conducted on SPEI drought analysis (Vicente-Serrano *et al.*, 2010; Wang *et al.*, 2014). The SPEI is able to detect the onset and spatial and temporal variation of a drought consistently, and it may be recommended for operational drought monitoring (Vicente-Serrano *et al.*, 2010). However, the SPEI can only identify the number of months in a drought period by applying the common monthly SPEI application and cannot identify the days of drought. The several days of drought during a crucial vegetation growth period can lead to severe harmful effects. However, the daily SPEI can monitor and assess drought at all timescales, from daily, weekly, monthly, to any longer scale, that is, the daily drought index can fill a void in the capability to monitor the onset and duration of droughts (Lu *et al.*, 2013). As a result, development of the daily SPEI is urgently needed, the daily SPEI data for shorter scales or longer scales can monitor meteorological drought or hydrological drought, because calculation and application of the daily SPEI are similar to monthly SPEI which can identify different drought types (meteorological drought, agricultural drought and hydrological drought) according to multi-time scales (Wang *et al.*, 2014).

In China, the Huang-Huai-Hai (HHH) plain is a very important food production area (Shi *et al.*, 2014). Planting areas of wheat and maize in the North China Plain occupy approximately 45% and 33% of the total planting area in China (Guo *et al.*, 2010). However, the HHH plain is also very susceptible to drought (Chen *et al.*, 2011). Higher temperatures may increase the potential evapotranspiration and may result in an increased occurrence of drought (Sheffield and Wood, 2008). In the past few decades, climate variation has affected the hydrological cycle in many places around the world, including the HHH plain, which also much influence the occurrence and severity of the water deficit (Gao *et al.*, 2006; Huntington, 2006; Sheffield and Wood, 2008). In the region, several studies have focused on the relationship between the drought index and environmental factors, including soil water content, crop water stress, El Niño Southern Oscillation (ENSO) and so on (Chen *et al.*, 2011; Huang *et al.*, 2013; Wu *et al.*, 2014). However, to quantify drought risk and effectively adopt countermeasures of regional defence to adapt to drought, the characteristics of the variability and patterns of drought should be comprehensively understood in the HHH plain. Additionally, it is important to determine the spatial-temporal characteristics in droughts and understand whether the occurrence of drought is exacerbated under global warming in the HHH plain.

The goal of this study is to develop a daily SPEI calculation method and apply it to assess the drought characteristics (severity, duration and frequency) in the HHH plain. In this study, the interannual variability of drought characteristics were investigated for each meteorological station via Hovmöller diagrams, the trend changes of the drought characteristics were identified using the nonparametric Mann–Kendall test method, and finally, the spatial pattern of drought characteristics were analysed. The results of this study can provide an important technological support for drought planning and risk management of drought disaster.

2. Study area and data sources

The HHH plain is located in northern China (31–42°E, 114–121°N) and forms part of the alluvial plain developed by the Yellow River, the Huaihe River and the Haihe River. According to the topography and the principle of comprehensive agricultural zoning in China, the HHH plain was divided into four sub-regions, including the Taihang-yanshan mountains piedmont plain, the Ji-lu-yu low lying plain, Shandong hilly agroforestry region and the Huang-huai plain (Figure 1). Arable land is the main land use type in the HHH plain (Figure 2). In our study, 28 meteorological stations were selected (Table 1). The 28

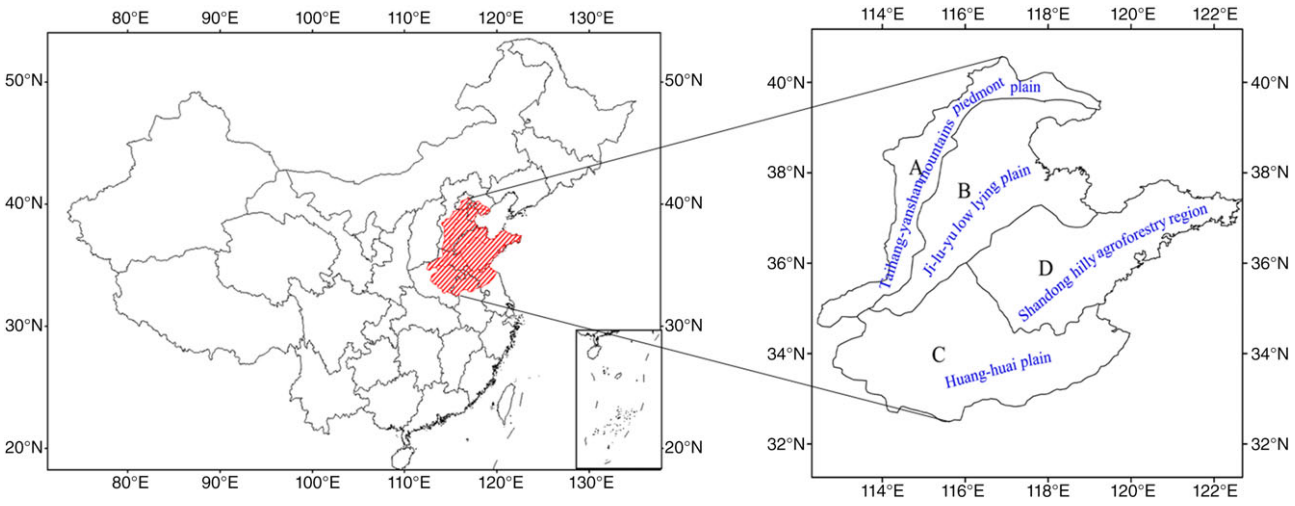

Figure 1. The study area (A: Taihang-yanshan mountains piedmont plain; B: Ji-lu-yu low lying plain; C: Shandong hilly agroforestry region; D: Huang-huai plain).

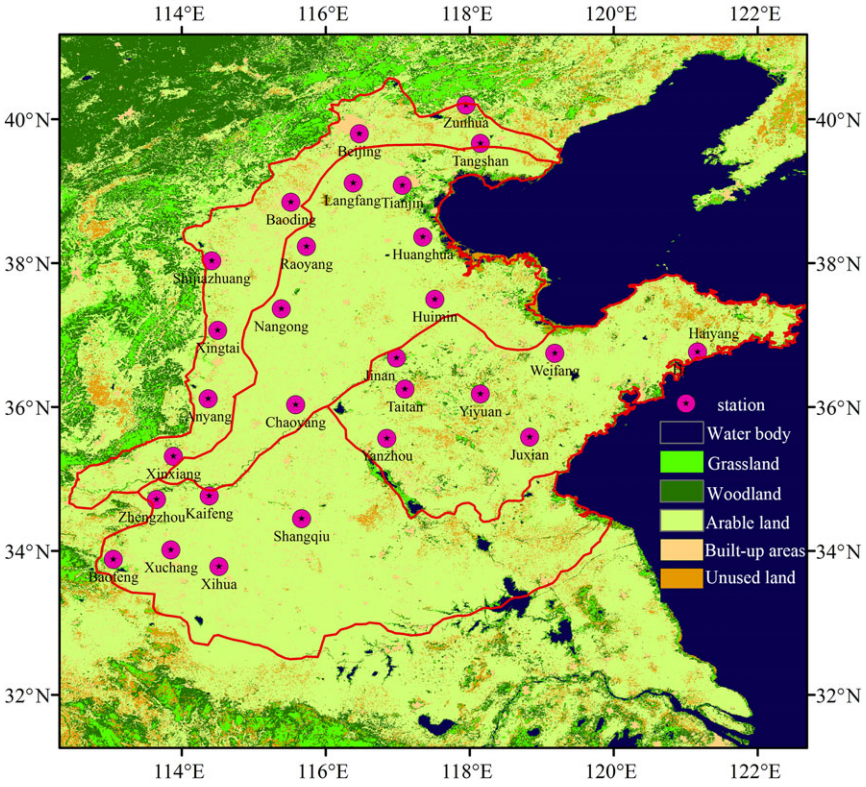

Figure 2. Spatial distribution of land use and the meteorological stations in the HHH plain (the circles denote the spatial distribution of the 28 meteorological stations; the rectangles in the legend identify the different land use types).

Table 1. Basic information about the 28 selected stations in the HHH plain.

Station name	Longitude (°E)	Latitude (°N)	Elevation (m)	Station name	Longitude (°E)	Latitude (°N)	Elevation (m)
Zunhua	117.95	40.20	55	Jinan	116.98	36.68	52
Beijing	116.47	39.80	31	Taishan	117.10	36.25	1534
Tangshan	118.15	39.67	28	Yiyuan	118.15	36.18	303
Langfang	116.38	39.12	9	Anyang	114.37	36.12	76
Tianjin	117.07	39.08	3	Chaoyang	115.58	36.03	43
Baoding	115.52	38.85	17	Juxian	118.83	35.58	107
Huanghua	117.35	38.37	7	Yanzhou	116.85	35.57	52
Raoyang	115.73	38.23	19	Xinxiang	113.88	35.32	73
Shijiazhuang	114.42	38.03	81	Kaifeng	114.38	34.77	73
Huimin	117.52	37.50	12	Zhengzhou	113.65	34.72	110
Nangong	115.38	37.37	27	Shangqiu	115.67	34.45	50
Xingtai	114.50	37.07	77	Xuchang	113.85	34.02	67
Haiyang	121.17	36.77	65	Baofeng	113.05	33.88	136
Weifang	119.18	36.75	22	Xihua	114.52	33.78	53

stations were evenly distributed throughout the HHH plain. Thus, the 28 selected stations can represent the spatial patterns of drought in the HHH plain.

Daily meteorological data from 1980 to 2010 of the selected stations were collected from the Chinese Meteorological Administration, including the minimum and maximum air temperature (°C), precipitation (mm) and sunshine duration (h). To ensure continuous and complete data records, we selected a total of 28 meteorological stations after dropping the stations with missing values for the period 1980–2010. Moderate Resolution Imaging Spectroradiometer (MODIS) land cover product (MCD12Q1) data with 500 m spatial resolution in 2010 were used, the data can be download from United States Geological Survey (USGS) (https://lpdaac.usgs.gov/products/modis_products_table/mcd12q1). The land use types were classified as six types: water body, grassland, woodland, arable land, built-up land and unused land (Liu *et al.*, 2003).

3. Methodology

3.1. Calculation of the SPEI

SPEI combines the precipitation data and the potential evapotranspiration calculation data; we followed

Hargreaves model approach to calculate the potential evapotranspiration. When wind speed, relative humidity and other data are completely absent, the potential evapotranspiration can also be estimated using the equation stated by Hargreaves and Samani (1982), which is given as:

$$\mathrm{PET} = 0.0023\ \left(T_{\mathrm{mean}} + 17.8\right)\ \sqrt{\left(T_{\max} - T_{\min}\right)}\, R_a \quad (1)$$

where PET is the daily potential evapotranspiration (mm/day); T_{mean} is the daily average air temperature (°C); $T_{\max}$ is the daily maximum air temperatures (°C); $T_{\min}$ is the daily minimum air temperatures (°C) and R_a is the net radiation at the surface (MJ m^{-2} day^{-1}).

In addition, when wind speed, relative humidity and other data are not completely absent, the above potential evapotranspiration estimated by other methods can be also replaced in calculation of the daily SPEI.

Solar radiation for Equation (1) at stations can be obtained by the sunshine duration based on the Ångström function (Jones, 1992). The net shortwave radiation is given by:

$$R_s = \left(a_s + b_s \frac{n}{N}\right) R_a \quad (2)$$

where R_s is net shortwave radiation (MJ m^{-2} day^{-1}), n is observed sunshine duration at stations (h), N is potential maximum sunshine duration (h), R_a is extraterrestrial radiation (MJ m^{-2} day^{-1}), a_s and b_s are constant, respectively 0.25 and 0.5.

The potential maximum sunshine duration (h) can be calculated using:

$$N = \left(\frac{24}{\pi}\right) \omega_s \quad (3)$$

where ω_s is sunset hour angle expressed in radians (rad), the calculation for ω_s may reference to Equation (5).

The extraterrestrial radiation, R_a for each day of the year and for different latitudes can be estimated from the solar constant, the solar declination and the time of the year by:

$$R_a = \frac{24 * 60}{\pi} G_{\mathrm{sc}} d_r \left[\left(\omega_s \sin\varphi \sin\delta\right) + \left(\cos\varphi \cos\delta \sin\omega_s\right)\right] \quad (4)$$

where G_{sc} is solar constant 0.0820 MJ m^{-2} min^{-1}, d_r is inverse relative distance Earth–Sun referencing to Equation (6), φ is latitude (rad), δ is solar declination (rad) which can be obtained by Equation (7).

$$\omega_s = \arccos\left[-\tan(\varphi)\tan(\delta)\right] \quad (5)$$

$$d_r = 1 + 0.033 \cos\left[\frac{2\pi}{365} J\right] \quad (6)$$

$$\delta = 0.409 \sin\left[\frac{2\pi}{365} J - 1.39\right] \quad (7)$$

where J is number of the day in the year between 1 (1 January) and 365 or 366 (31 December).

The deficit or surplus accumulation of a climate water balance at different time scales is determined by the difference between the precipitations (P) and PET for the day i:

$$D_i = P_i - \mathrm{PET}_i \quad (8)$$

The calculated D_i values are aggregated at different time scales, following the same procedure as that for the SPI. The difference $D_{i,j}^k$ in a given day j and year i depends on the chosen time scale k (days). For example, the accumulated difference for 1 day in a particular year i with a 90-day time scale is calculated using:

$$X_{i,j}^k = \sum_{l=91-k+j}^{90} D_{i-1,l} + \sum_{l=1}^{j} D_{i,l}, \text{ if } j < k \text{ and}$$

$$X_{i,j}^k = \sum_{l=j-k+1}^{j} D_{i,l}, \qquad \text{if } j \geq k. \quad (9)$$

Next, normalize the water balance into a log–logistic probability distribution to obtain the SPEI index series. The log–logistic distribution was selected for standardizing the D series to obtain the SPEI. The probability density function of a log–logistic distributed variable is expressed as:

$$f(x) = \frac{\beta}{\alpha}\left(\frac{\chi - \lambda}{\alpha}\right)\left[1 + \left(\frac{\chi - \lambda}{\alpha}\right)\right]^{-2} \quad (10)$$

where α, β, and γ are the scale, shape and origin parameters, respectively, for D values in the range ($\gamma > D < \infty$).

Thus, the probability distribution function of the D series is given by:

$$F(x) = \left[1 + \left(\frac{\alpha}{\chi - \gamma}\right)^{\beta}\right]^{-1} \quad (11)$$

With $F(x)$, the SPEI can easily be obtained as the standardized values of $F(x)$. Following the classical approximation of Abramowitz and Stegun (1965):

$$\mathrm{SPEI} = W - \frac{C_0 + C_1 W + C_2 W^2}{1 + d_1 W + d_2 W^2 + d_3 W^3} \quad (12)$$

where $W = \sqrt{-2\ln(P)}$ for $P \leq 0.5$ and P is the probability of exceeding a determined D value, $P = 1 - F(x)$. If $P > 0.5$, then P is replaced by $1 - P$ and the sign of the resultant SPEI is reversed. The constants are $C_0 = 2.515517$, $C_1 = 0.802853$, $C_2 = 0.010328$, $d_1 = 1.432788$, $d_2 = 0.189269$ and $d_3 = 0.001308$.

3.2. Trend analysis method

The Mann–Kendall (MK) trend test (Mann, 1945; Kendall, 1975) is a rank-based nonparametric test for assessing the significance of a trend and has been widely used in hydro-meteorological trend detection studies (Burn and Hag Elnur, 2002; Xu *et al.*, 2004). The null hypothesis H0 is that a sample of data (X_i, $i = 1, 2, \ldots n$) is independent and identically distributed. The alternative hypothesis H1 is that a monotonic trend exists in X. The MK test statistic is calculated as:

$$S = \sum_{i=1}^{n-1} \sum_{i=j+1}^{n} sgn\left(x_j - x_i\right) \quad (13)$$

where the x_j are the sequential data values, n is the length of the data set, and

$$sgn\left(x_j - x_i\right) = \begin{cases} 1 & if \quad x_j > x_i \\ 0 & if \quad x_j = x_i \\ -1 & if \quad x_j < x_i \end{cases} \tag{14}$$

Mann (1945) and Kendall (1975) documented that when $n \geq 8$, the statistic S is approximately normally distributed, with the mean and the variance as follows:

$$E(S) = 0 \tag{15}$$

$$V(S) = \frac{n(n-1)(2n+5) - \sum_{m=1}^{n} t_m m(m-1)(2m+5)}{18} \tag{16}$$

where t_m is the number of extent m. The standardized test statistic Z is computed by

$$Z = \begin{cases} \frac{S-1}{\sqrt{V(S)}} & S > 0 \\ 0 & S = 0 \\ \frac{S+1}{\sqrt{V(S)}} & S < 0 \end{cases} \tag{17}$$

When the significance levels are set at 0.01, 0.05, and 0.1 and $|Z_\alpha|$ are 2.58, 1.96 and 1.65, respectively. At a certain significance level, if $|Z| > |Z_\alpha|$, then the null hypothesis H0 is rejected. In this article, the significance levels of $p = 0.05$ and 0.01 are discussed.

3.3. Data processing

The 90-day (3-month) time scale for the SPEI can monitor soil moisture and agriculture drought (Wang *et al.*, 2014), and the daily SPEI data were calculated for the 90-day time scale using the daily precipitation and air temperature data from 1981 to 2010 at 28 station locations. The classifications for the SPEI drought class are presented in Table 2.

We investigated the drought characteristics of the variability and pattern of drought severity, drought duration and drought frequency. To define the drought-related variables, we adapted the run model described by Yevjevich *et al.* (1967). Once a drought event was determined with its start and end day, its duration and severity were then assigned. Considering the continuity of drought properties, we defined continuous days with SPEI values less than −0.5 as a drought event at each station, and the end of a drought event is defined as the day the SPEI is greater than or equal to −0.5. The severity is the absolute value of the integral area between the SPEI line (value < −0.5) and the horizontal axis (SPEI = 0) from the start to the end day of a drought event; the greater value the integral area for a drought event, the more severe the drought is. The duration of a drought event is equal to the number of days between its start (included) and end day (not included), because for defining a drought event according to Table 2, the end day cannot be included in drought event when SPEI is great than −0.5. The frequency is defined as the number of drought events in a given period.

Table 2. Classification used for the SPEI (McKee *et al.*, 1993; Paulo *et al.*, 2012).

Drought class	SPEI values
Non-drought	SPEI ≥ −0.5
Mild	−1 < SPEI < −0.5
Moderate	−1.5 < SPEI ≤ −1
Severe	−2 < SPEI ≤ −1.5
Extreme	SPEI ≤ −2

To assess the variability and pattern of the drought characteristics, the values of Annual Total Drought Severity (ATDS), Annual Total Drought Duration (ATDD) and Annual Drought Frequency (ADF) were then computed for at every station between 1981 and 2010. In the maps, ATDS is obtained by summing the severity of the drought events in every year, ATDD is obtained by summing the duration of the drought events in every year, and ADF is calculated by summing number of the drought events in every year. ATDS is a dimensionless drought severity score, ATDD is expressed in number of days and ADF is expressed as the number of events in every year.

In our study, Spatial-Time (Hovmöller) diagrams (Hovmöller, 1949) were used to investigate the interannual variability of drought characteristics at 28 stations, which can present the data in a spatial-temporal cross-section. The MK trend test was applied for the existence of a trend of ATDS, ATDD and ADF. Finally, the spatial patterns of drought characteristics were investigated by averaging the values of ATDS, ATDD and ADF at the 28 stations of our study. The average values for each station are compared with those for the entire study area.

4. Results and discussion

4.1. Interannual variability of drought characteristics

The interannual variability of severe drought areas can identify the severe drought year and the spatial distribution of severe drought in the study area. The daily SPEI data on a 90-day scale for each year are used to study the interannual variability of drought characteristics at 28 stations in the HHH plain. The most severe drought years are identified based on the interannual variability of drought characteristics.

The interannual variability of drought characteristics between 1981 and 2010 is shown in Figure 3 in form of Hovmöller diagrams of ATDS, ATDD and ADF. Figure 3 shows the remarkable interannual variability of the drought characteristics for each station.

The interannual variability of drought characteristics for the near stations is similar, as shown in Figure 3(a) and (b), which may be due to wide range of environmental conditions, including precipitation and temperature. Figure 3(a) and (b) show that the most serious ATDS and the longest ATDD of drought occurred in 1981, 1986, 1997 and 2002 for nearly all of the stations, with the drought duration exceeding 190 days in the severe drought years. We can

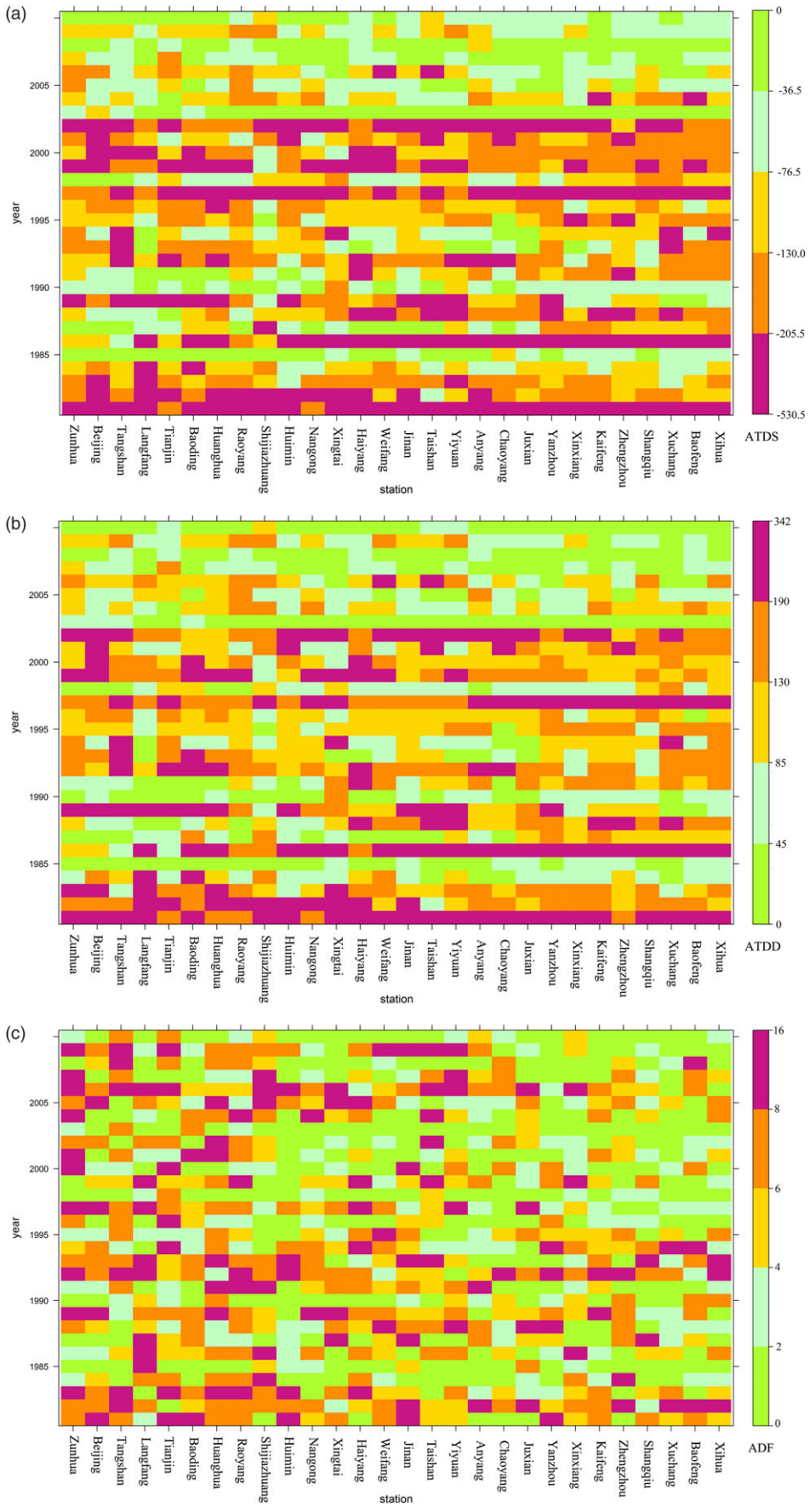

Figure 3. Hovmöller diagrams for ATDS (a), ATDD (b) and ADF (c) at 28 meteorological stations (the horizontal axis indicates the station names and the vertical axis indicates the year from 1981 to 2010; the stations are listed from north to south in HHH plain in the horizontal axis).

also identify the years (in 1985, 1990, 2003, 2008 and 2010) of the least serious ATDS and the shortest ATDD in the HHH plain. These results demonstrate that the variations of drought severity and drought duration were in agreement, which may be attributed to the fact that a long duration of drought is a basis of severe drought formation. Since 2003, both weak ATDS and weak ATDD occurred in the entire HHH Plain. To some extent, if ATDS and ATDD are serious, the corresponding drought will be severe drought. Thus, severe drought came in the 1980s, late 1990s and early 2000s; in particular, drought events in 1981, 1986, 1997 and 2002 are very severe. In 1997, the serious drought and hot summer were attributed to the weak Asian summer monsoon influenced by the ENSO cycle (Huang *et al.*, 2000), while the 2002 drought event was caused by the shortage of the rainfall in rainy season (Dai *et al.*, 2003). We also identified the years of severe drought that depend on our interannual variability of drought characteristics. The above reported drought events in the HHH plain can test the effectiveness of the identification. Figure 3(c) also shows that the Spatial-temporal characteristics of ADF do not agree with those of the ATDS and ATDD. The dispersed distribution characteristics for ADF are shown in Figure 3(c), that is, near stations have obviously different values of ADF in the same year, which is probably due to some regions experiencing light rainfall that disturbed an otherwise continuously widespread drought; we also find that the variation in the northern region is greater than in the southern region for the entire HHH plain and that the northern region is more prone to drought than the southern region.

4.2. Variation trend of drought in HHH

The MK test method is applied to analyse the trends of ATDS, ATDD and ADF of the drought characteristics at the 28 stations of this study from 1981 to 2010. The changes of the trends using the MK test are illustrated in Figure 4.

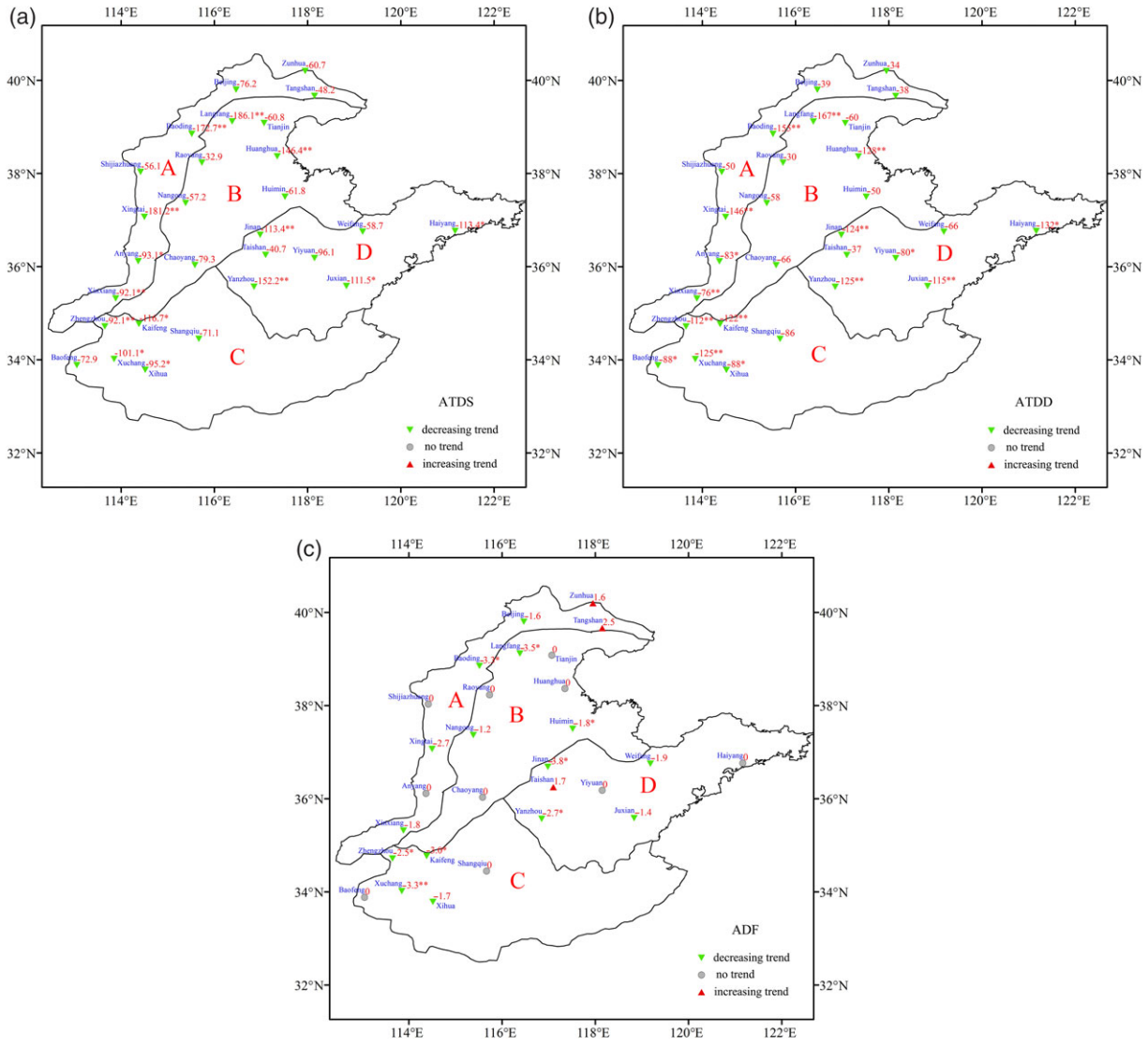

Figure 4. The single-site trend analysis for ATDS (a), ATDD (b) and ADF (c) at 28 meteorological stations (letter (A, B and C) represent the change trend per 30 year, symbol (**) following the numbers represents a significance level of $p = 0.01$, symbol (*) represents the significance level of 0.05).

ATDS may indicate severity of drought for each year, and Figure 4(a) shows that a decreasing trend of ATDS is found at all stations in the past 30 years. The smaller the value of ATDS, the more severe drought occurred. More significant trends for the ATDS at the 0.01 significance levels are observed at the Langfang, Baoding and Huanghua stations in the northern regions of the HHH plain, and six stations are at the 0.05 significance levels, where increasing trends for ATDS demonstrated that the drought severity was moderating.

A decreasing trend for ATDD was found at all stations in Figure 4(b), i.e. the numbers of the drought duration days exhibit a decreasing tendency, and more significant trends for ATDS at 0.01 significance levels are also observed at the Langfang, Baoding, Huanghua stations in the northern regions of the HHH plain and five stations at 0.05 significance levels. The trend changes for ATDD demonstrate that drought is alleviating at all of the stations.

ADF is shown in Figure 4(c), there are 15 stations with a decreasing trend for ADF, and the other 13 stations include 10 stations without a change trend and 3 stations with an increasing trend. The decreasing trend for ATDS at Xuchang station is at the 0.01 significance level, seven stations are at 0.05 significance levels and no station with an increasing trend is at 0.01 or 0.05 significance levels. The trend changes for ADF demonstrated that the numbers of drought events for each year do not obviously increase in the past 30 years.

Trend changes of drought severity, duration and frequency are in agreement: the results of this study indicated weakening droughts in the HHH plain, which may be attributed to increased rainfall under warming temperature (Wu *et al.*, 2014). The increasing rainfall effect on drought alleviation is probably partially offset by the warming effect. The trend changes for ATDS, ATDD and ADF do not exhibit the difference between sub-regions of the HHH plain, probably because there are similar topographies and land use types among the sub-regions.

By investigating the trend changes for the ATDS, ATDD and ADF of the drought characteristics, the results of this study indicated weakening droughts in the HHH plain, which may be attributed to increasing aerosols that decreased the solar radiation and reduced the potential evapotranspiration (Gao *et al.*, 2006). In light of global warming and climate change, the changing trends of droughts in the HHH plain are likely to continue and the drought situation will be alleviated.

4.3. Spatial pattern of the drought characteristics

To quantitatively evaluate the spatial variance of the drought characteristics, we use the above spatial pattern analysis method. The multi-year averaging values of ATDS, ATDD and ADF for each station can demonstrate the spatial variance of drought characteristics. Table 3 provides spatial comparisons of the mean ATDS, mean ATDD

Table 3. Spatial pattern analysis for the mean ATDS, ATDD and ADF at 28 meteorological stations.

Station name	Longitude (°E)	Latitude (°N)	Mean (ATDS)	Mean (ATDD)	Mean (ADF)	Sub-region
Zunhua	117.95	40.20	**131.66**	**117**	**6.00**	A
Beijing	116.47	39.80	126.96	113	**4.87**	A
Tangshan	118.15	39.67	**132.31**	**118**	**5.57**	A
Langfang	116.38	39.12	124.83	110	**5.57**	B
Tianjin	117.07	39.08	129.46	111	**5.73**	B
Baoding	115.52	38.85	**134.61**	**119**	4.47	A
Huanghua	117.35	38.37	**135.43**	120	**5.97**	B
Raoyang	115.73	38.23	128.75	112	**5.53**	B
Shijiazhuang	114.42	38.03	125.65	112	**5.53**	A
Huimin	117.52	37.50	129.24	111	4.30	B
Nangong	115.38	37.37	122.72	105	4.70	B
Xingtai	114.50	37.07	130.12	114	4.33	A
Haiyang	121.17	36.77	**136.10**	**120**	**4.90**	D
Weifang	119.18	36.75	**134.58**	**117**	4.50	D
Jinan	116.98	36.68	131.48	113	**4.77**	D
Taishan	117.10	36.25	130.57	113	**4.90**	D
Yiyuan	118.15	36.18	**134.42**	**119**	**4.80**	D
Anyang	114.37	36.12	**133.35**	**115**	4.07	A
Chaoyang	115.58	36.03	128.10	106	3.97	B
Juxian	118.83	35.58	**132.06**	113	4.57	D
Yanzhou	116.85	35.57	**133.69**	**115**	4.30	D
XinXiang	113.88	35.32	128.52	110	4.60	A
Kaifeng	114.38	34.77	**135.10**	**119**	4.13	C
Zhengzhou	113.65	34.72	131.72	113	4.50	C
Shangqiu	115.67	34.45	131.29	114	3.77	C
Xuchang	113.85	34.02	**136.69**	**118**	3.60	C
Baofeng	113.05	33.88	**132.08**	112	4.20	C
Xihua	114.52	33.78	**135.24**	**117**	4.27	C
The mean value in the entire HHH plain			131.31	114	4.73	

Bold values indicates that the multi-year averaging values is greater than the mean of the entire study area.

and mean ADF of the drought characteristics from 1981 to 2010.

Figure 2 and Table 3 indicate that the stations for ATDS are mainly distributed in the northwest regions of the study area, and the stations in the northeast and southwest are greater in the entire HHH plain. There are lower values for the mean ATDS, except for HuangHua station in the Ji-lu-yu low lying plain (region B). The station for ATDD with the longest duration (120 days) is Haiyang, and the station with the shortest duration is Nangong (105 days); the stations with longer ATDD also have a greater ATDS, and the stations with (ATDD > 114 days) are Zunhua, Tangshan, Baoding, Haiyang, Weifang, Yiyuan, Anyang, Yanzhou, Kaifeng, Xuchang and Xihua. The drought events are found to have greater drought severity and the longest drought duration. The results of the pattern for the mean ATDS and the mean ATDD demonstrate that the northeast and southwest regions of the HHH plain suffered from more severe drought. Figure 2 and Table 3, the data indicate that the stations for greater ADF with most drought events (>4.7) are mainly distributed in the north of the whole HHH plain. There are no stations with a greater ADF in region C; this result implies that the north region of HHH plain is prone to drought. The spatial distribution of drought frequency in the HHH plain is consistent with a previous study (Yu *et al.*, 2014). The regions that are prone to drought should cultivate drought-tolerant crop species and strengthen the construction of water conservancy irrigation facilities.

5. Conclusion

The variability and pattern of the drought characteristics are one of the most important aspects of drought disaster mitigation. On the basis of daily Standardized Precipitation Evaporation Index, in this study, the no-parameter MK trend test was applied to assess the variability and pattern of drought characteristic in the HHH plain from 1981 to 2010. Using ATDS, ATDD and ADF as the main assessing indicators, we investigated the variability and pattern of the drought characteristics in the entire HHH plain and its four sub regions. Severe drought events may cause serious impact in some years. Using the Hovmöller diagrams, the severe drought events are identified by analysing the interannual variability of drought characteristics in the HHH plain, and regions that were prone to severe drought were identified on the basis of the variability and pattern analysis.

The severe drought years can be identified by both the ATDS and ATDD and that severe drought occurred in the 1980s, late 1990s and early 2000s; in particular, the drought events in 1981, 1986, 1997 and 2002 were very severe. The interannual variations of ATDS and ATDD were in agreement among the different nearby stations, while the nearby stations had obviously different values of ADF in the same year. The trend changes of drought severity, drought duration and drought frequency were in agreement with the wet climate environment tendency and the alleviating drought situation. Although the drought situation is changing, the northeast and southwest regions of the HHH plain are suffering from more severe drought, and the north region with most drought events (>4.7) is prone to drought.

These conclusions can provide a scientific understanding for the management of drought mitigation strategies on a regional scale. Identifying the drought-prone areas can help decision makers to take drought into account in resource planning in drought-prone areas. However, it is better to apply the developed daily SPEI to drought events in reality; in addition, our study adopted the SPEI data obtained from stations, which probably influences certain spatial descriptions of drought characteristics in detail.

Acknowledgements

This research received financial support from the International Science & Technology Cooperation Programme of China (grant numbers: 2013DFG21010 and 2012DFG21710-03), and also supported by "the Fundamental Research Funds for the Central Universities". The authors have declared no conflicting interests. The authors thank Stagge, J.H. for the SPEI developed calculation. We would like to thank Bin He, Zhitao Wu, Guangyu Li for providing helpful editorial support and the reviewers of the manuscript for their helpful comments.

References

Abramowitz M, Stegun I. 1965. *Handbook of Mathematical Functions, with Formulas, Graphs, and Mathematical Tables*. Dover: New York, NY, 1046 pp.

Banimahd SA, Khalili D. 2013. Factors influencing Markov chains predictability characteristics, utilizing SPI, RDI, EDI and SPEI drought indices in different climatic zones. *Water Resour. Manage.* **27**: 3911–3928.

Blunden J, Arndt D, Baringer M. 2011. State of the climate in 2010. *Bull. Am. Meteorol. Soc.* **92**: S1–S236.

Bruins HJ, Berliner PR. 1998. Bioclimatic aridity, climatic variability, drought and desertification: definitions and management options. In *The Arid Frontier*, Bruins HJ, Lithwick H (eds). Springer: Houten, Netherlands, 97–116.

Burn DH, Hag Elnur MA. 2002. Detection of hydrologic trends and variability. *J. Hydrol.* **255**: 107–122.

Chen J, Wang C, Jiang H, Mao L, Yu Z. 2011. Estimating soil moisture using Temperature–Vegetation Dryness Index (TVDI) in the Huang-huai-hai (HHH) plain. *Int. J. Remote Sens.* **32**: 1165–1177.

Dai X, Wang P, Chou J. 2003. Multiscale characteristics of the rainy season rainfall and interdecadal decaying of summer monsoon in North China. *Chin Sci. Bull.* **48**: 2730–2734.

Dubrovsky M, Svoboda M, Trnka M, Hayes M, Wilhite D, Zalud Z, Hlavinka P. 2009. Application of relative drought indices in assessing climate-change impacts on drought conditions in Czechia. *Theor. Appl. Climatol.* **96**: 155–171.

Gao G, Chen D, Ren G, Chen Y, Liao Y. 2006. Spatial and temporal variations and controlling factors of potential evapotranspiration in China: 1956–2000. *J. Geogr. Sci.* **16**: 3–12, doi: 10.1007/s11442-006-0101-7.

Guo R, Lin Z, Mo X, Yang C. 2010. Responses of crop yield and water use efficiency to climate change in the North China Plain. *Agric. Water Manage.* **97**: 1185–1194.

Guttman NB. 1998. Comparing the palmer drought index and the standardized precipitation index. *J. Am. Water. Resour. Assoc.* **34**: 113–121.

Hagman G, Beer H, Bendz M, Wijkman A. 1984. *Prevention Better Than Cure. Report on Human and Environmental Disasters in the Third World*, 2nd edn. Swedish Red Cross: Stockholm.

Hargreaves GH, Samani ZA. 1982. Estimating potential evapotranspiration. *J. Irrig. Drain. Div.* **108**: 225–230.
Hayes MJ, Svoboda MD, Wilhite DA, Vanyarkho OV. 1999. Monitoring the 1996 drought using the standardized precipitation index. *Bull. Am. Meteorol. Soc.* **80**: 429–438.
He B, Lü A, Wu J, Zhao L, Liu M. 2011. Drought hazard assessment and spatial characteristics analysis in China. *J. Geogr. Sci.* **21**: 235–249.
Hovmöller E. 1949. The Trough-and-Ridge diagram. *Tellus* **1**: 62–66.
Hu Y, Liang Z, Yong W, Wang J, Yao L, Ning Y. 2014. Uncertainty analysis of SPI calculation and drought assessment based on the application of Bootstrap. *Int. J. Climatol.*, doi: 10.1002/joc.4091.
Huang R, Zhang R, Zhang Q. 2000. The 1997/98 ENSO cycle and its impact on summer climate anomalies in East Asia. *Adv. Atmos. Sci.* **17**: 348–362.
Huang Y, Tian Q, Du L, Sun S. 2013. Analysis of spatial-temporal variation of agricultural drought and its response to ENSO over the past 30 years in the Huang-Huai-Hai region, China. *Terr. Atmos. Ocean. Sci.* **24**: 745–759.
Huntington TG. 2006. Evidence for intensification of the global water cycle: review and synthesis. *J. Hydrol.* **319**: 83–95.
Jones HG. 1992. *Plant and Microclimate. A Quantitative Approach to Environmental Plant Physiology*, 2nd edn. Cambridge University Press: Cambridge, UK, 428 pp.
Kendall M. 1975. *Rank Correlation Measures*. Charles Griffin: London, 202.
Leuzinger S, Zotz G, Asshoff R, Körner C. 2005. Responses of deciduous forest trees to severe drought in Central Europe. *Tree Physiol.* **25**: 641–650.
Li X, Jiang F, Li L, Wang G. 2011. Spatial and temporal variability of precipitation concentration index, concentration degree and concentration period in Xinjiang, China. *Int. J. Climatol.* **31**: 1679–1693, doi: 10.1002/joc.2181.
Liu C, Zhang S. 2002. Drying up of the yellow river: its impacts and counter-measures. *Mitig. Adapt. Strateg. Glob. Change* **7**: 203–214.
Liu J, Liu M, Zhuang D, Zhang Z, Deng X. 2003. Study on spatial pattern of land-use change in China during 1995–2000. *Sci. Chin. Ser. D: Earth Sci.* **46**: 373–384.
Lu E, Cai W, Jiang Z, Zhang Q, Zhang C, Higgins RW, Halpert MS. 2013. The day-to-day monitoring of the 2011 severe drought in China. *Clim. Dyn.* **43**: 1–9.
MacDonald GM. 2007. Severe and sustained drought in southern California and the West: present conditions and insights from the past on causes and impacts. *Quat. Int.* **173**: 87–100.
Mann HB. 1945. Nonparametric tests against trend. *Econometrica* **13**: 245–259.
McKee TB, Doesken NJ, Kleist J. 1993. The relationship of drought frequency and duration to time scales. In *Proceedings of the 8th Conference on Applied Climatology*. American Meteorological Society: Boston, MA, 179–183.
Palmer WC. 1965. Meteorological drought, Research Paper No. 45, US Department of Commerce, Weather Bureau, Washington, DC.
Paulo A, Rosa R, Pereira L. 2012. Climate trends and behaviour of drought indices based on precipitation and evapotranspiration in Portugal. *Nat. Hazards Earth Syst. Sci.* **12**: 1481–1491.
Pausas JG. 2004. Changes in fire and climate in the eastern Iberian Peninsula (Mediterranean basin). *Clim. Change* **63**: 337–350.
Quiring SM, Papakryiakou TN. 2003. An evaluation of agricultural drought indices for the Canadian prairies. *Agric. For. Meteorol.* **118**: 49–62.
Rhee J, Im J, Carbone GJ. 2010. Monitoring agricultural drought for arid and humid regions using multi-sensor remote sensing data. *Remote Sens. Environ.* **114**: 2875–2887.
Sheffield J, Wood EF. 2008. Global trends and variability in soil moisture and drought characteristics, 1950–2000, from observation-driven simulations of the terrestrial hydrologic cycle. *J. Clim.* **21**: 432–458.
Sheffield J, Wood EF, Roderick ML. 2012. Little change in global drought over the past 60 years. *Nature* **491**: 435–438.
Shen C, Wang W-C, Hao Z, Gong W. 2007. Exceptional drought events over eastern China during the last five centuries. *Clim. Change* **85**: 453–471.
Shi W, Tao F, Liu J. 2014. Regional temperature change over the Huang-Huai-Hai Plain of China: the roles of irrigation versus urbanization. *Int. J. Climatol.* **34**: 1181–1195.
Vicente-Serrano SM, Beguería S, López-Moreno JI, Angulo M, El Kenawy A. 2010. A new global 0.5 gridded dataset (1901–2006) of a multiscalar drought index: comparison with current drought index datasets based on the Palmer Drought Severity Index. *J. Hydrometeorol.* **11**: 1033–1043.
Wang A, Lettenmaier DP, Sheffield J. 2011. Soil moisture drought in China, 1950–2006. *J. Clim.* **24**: 3257–3271.
Wang Q, Wu J, Lei T, He B, Wu Z, Liu M, Mo X, Geng G, Li X, Zhou H, Liu D. 2014. Temporal-spatial characteristics of severe drought events and their impact on agriculture on a global scale. *Quat. Int.* **349**: 10–21.
Wilhite DA. 1996. A methodology for drought preparedness. *Nat. Hazards* **13**: 229–252.
Wilhite DA (ed). 2000. Drought as a natural hazard: concepts and definitions. In *Drought: A Global Assessment*, Vol. **1**. Routledge Publishers: London, 3–18.
Wilhite DA, Svoboda MD, Hayes MJ. 2007. Understanding the complex impacts of drought: a key to enhancing drought mitigation and preparedness. *Water Resour. Manage.* **21**: 763–774.
Wu J, Zhou L, Liu M, Zhang J, Leng S, Diao C. 2013. Establishing and assessing the Integrated Surface Drought Index (ISDI) for agricultural drought monitoring in mid-eastern China. *Int. J. Appl. Earth Obs. Geoinf.* **23**: 397–410.
Wu J, Liu M, Lü A, He B. 2014. The variation of the water deficit during the winter wheat growing season and its impact on crop yield in the North China Plain. *Int. J. Biometeorol.* **58**: 1951–1960.
Xu Z, Chen Y, Li J. 2004. Impact of climate change on water resources in the Tarim River basin. *Water Resour. Manage.* **18**: 439–458.
Yevjevich V, Ingenieur J, Yevjevich V, Ingénieur Y, Yevjevich V, Engineer Y. 1967. *An Objective Approach to Definitions and Investigations of Continental Hydrologic Droughts*. Colorado State University: Fort Collins, CO.
Yu M, Li Q, Hayes MJ, Svoboda MD, Heim RR. 2014. Are droughts becoming more frequent or severe in China based on the standardized precipitation evapotranspiration index: 1951–2010? *Int. J. Climatol.* **34**: 545–558.
Zhang Q, Sun P, Li J, Singh VP, Liu J. 2014. Spatiotemporal properties of droughts and related impacts on agriculture in Xinjiang, China. *Int. J. Climatol.*, doi: 10.1002/joc.4052.

